IEEE Access
Multidisciplinary | Rapid Review | Open Access Journal

Received May 1, 2018, accepted June 20, 2018, date of publication June 25, 2018, date of current version July 12, 2018.

Digital Object Identifier 10.1109/ACCESS.2018.2850055

High Velocity Motion Compensation of IFDS Data in ISAR Imaging Based on Adaptive Parameter Adjustment of Matched Filter and Entropy Minimization

BIAO TIAN, ZHEJUN LU, YONGXIANG LIU, (Member, IEEE), AND XIANG LI, (Member, IEEE)
College of Electronic Science, National University of Defense Technology, Changsha 410073, China

Corresponding author: Biao Tian (tbncsz@nudt.edu.cn)

This work was supported in part by the National Natural Science Foundation of China under Grant 61501481 and Grant 61571449, in part by the Hunan Province Innovation Foundation for Postgraduates under Grant CX2014B020, and in part by the National University of Defense Technology Innovation for Excellent Postgraduates under Grant B140405.

ABSTRACT This paper proposes a new high-velocity motion compensation method for intermediate frequency direct sampling (IFDS) data by adaptive parameter adjustment of a matched filter and entropy minimization. First, the influence of high-velocity motion to IFDS data is analyzed. The high-velocity motion brings in aberration to the range profile and blurring the phase of inverse synthetic aperture radar imaging. Then, adaptive parameter adjustment of a matched filter is designed to accomplish joint high-velocity motion compensation and pulse compression. The iterative search for the velocity utilizing golden section search based on waveform entropy minimization is adopted to improve the efficiency. Experimental results demonstrate the validity of the proposed method.

INDEX TERMS Inverse synthetic aperture radar, high velocity motion compensation, intermediate frequency direct sampling, entropy minimization, golden section search.

I. INTRODUCTION

Inverse synthetic aperture radars (ISARs) are extensively used in military and civilian applications because they can generate two-dimensional (2-D) high-resolution images of long-distance non-cooperative targets, under all weather conditions [1]–[4].

When the relative radial velocity of the radar and the target is very small, it is considered that the distance between the radar and the target is almost invariable in the duration of radar pulse. It is just the 'stop-go-stop' hypothesis which is commonly used in air target ISAR imaging. However, the relative radial velocity of the space orbit object is as large as several kilometers per second. The hypothesis is no longer valid. In the process of space object ISAR imaging, the high velocity radial motion of the object results in one dimensional (1-D) range profile aberration and two dimensional (2-D) ISAR image blurring. Because of the principle difference between the Fourier transform (FT) based pulse compression for Dechirp data and the matched filter based pulse compression for intermediate frequency direct sampling (IFDS) data [5], the mechanism of the high velocity motion of the target is not the same to them.

The research of high velocity motion analysis and compensation method for Dechirp signals is very mature [6]–[8]. Usually, the target radial velocity is estimated by means of signal processing, and then the high-order phase caused by the radial velocity in the Dechirp echo is compensated to accomplish the high velocity motion compensation. Unlike the Dechirp echo, the velocity disturbance phase of the IFDS echo is coupled with the target rotation phase, which cannot be separated. Hence, the compensation method for Dechirp echo cannot be applied any more.

Aiming at the high velocity motion compensation of IFDS data problem, a new method based on adaptive parameter adjustment of matched filter and entropy minimization is proposed in this paper. The remainder of this paper is organized as follows. In Section II, the ISAR imaging signal model of IFDS data with high velocity motion is described. Section III analyzes the high velocity motion compensation method based on adaptive parameter adjustment of matched

filter and entropy minimization. Section IV reports the simulation and real data performance analysis, and Section V concludes the paper.

II. SIGNAL MODELING OF ISAR IMAGING WITH HIGH VELOCITY MOTION

Suppose the transmitting LFM signal is

$$s(\hat{t}, t_m) = \text{rect}\left(\frac{\hat{t}}{T_p}\right) \exp\left\{j2\pi\left(f_c t + \frac{1}{2}\gamma\hat{t}^2\right)\right\}, \quad (1)$$

where T_p is pulse width, f_c is carrier frequency, γ is the frequency modulation rate (FMR), $t_m = mT$ $(m = 0, 1, 2, \cdots)$ is slow time, $\hat{t}$ is fast time, and

$$\text{rect}(u) = \begin{cases} 1 & |u| \le 0.5 \\ 0 & |u| > 0.5. \end{cases} \quad (2)$$

In this paper, the point scattering model is applied to the radar echo. Suppose the target has N scattering centers, the range history of the k^{th} scattering center to antenna at time $(\hat{t}, t_m)$ can be expressed as

$$R_k(\hat{t}, t_m) = R_k(t_m) + V_{Tran}\hat{t} \quad 1 \le k \le N, \quad (3)$$

Then the received base band signal after quadrature demodulation is

$$\begin{aligned} s_{IF}(\hat{t}, t_m) = &\sum_{k=1}^{N} \sigma_k \text{rect}\left(\frac{\hat{t} - 2\left(R_k\left(t_m\right) + V_{Tran}\hat{t}\right)/c}{T_p}\right) \\ &\cdot \exp\left\{j\pi\gamma\left(\hat{t} - \frac{2\left(R_k\left(t_m\right) + V_{Tran}\hat{t}\right)}{c}\right)^2\right\} \\ &\cdot \exp\left\{-j2\pi f_c \frac{2\left(R_k\left(t_m\right) + V_{Tran}\hat{t}\right)}{c}\right\}, \end{aligned} \quad (4)$$

where σ_k is the scattering coefficient of k^{th} scattering center and c is the light speed.

Let us denote

$$\begin{aligned} a &= 1 - 2V_{Tran}/c \\ \tau_k &= 2R_k\left(t_m\right)/c. \end{aligned} \quad (5)$$

Then (4) can be rewritten as

$$\begin{aligned} s_{IF}(\hat{t}, t_m) = &\sum_{k=1}^{N} \sigma_k \text{rect}\left(\frac{a\hat{t} - \tau_k}{T_p}\right) \cdot \exp\left\{j\pi\gamma\left(a\hat{t} - \tau_k\right)^2\right\} \\ &\cdot \exp\left\{-j2\pi f_c \tau_k\right\} \cdot \exp\left\{-j2\pi f_c\left(1 - a\right)\hat{t}\right\}. \end{aligned} \quad (6)$$

If the complex conjugate of echo from stationary point target is used as the reference signal of matched filtering, namely

$$h\left(\hat{t}\right) = \text{rect}\left(\frac{\hat{t}}{T_p}\right) \exp\left\{-j\pi\gamma\hat{t}^2\right\}. \quad (7)$$

Hence the range profile after matched filtering can be obtained.

$$\begin{aligned} &s_{out}(\hat{t}, t_m) \\ &= s_{IF}(\hat{t}, t_m) \otimes h(\hat{t}) \\ &= \int_{-\infty}^{+\infty} h(\hat{t} - u) \cdot s_{IF}(u, t_m) du \\ &= \int_{-\infty}^{+\infty} \left\{\text{rect}\left(\frac{\hat{t} - u}{T_p}\right) \cdot \exp\left\{-j\pi\gamma(\hat{t} - u)^2\right\}\right. \\ &\qquad \cdot \text{rect}\left(\frac{au - \tau_k}{T_p}\right) \\ &\qquad \left. \cdot \exp\left\{-j2\pi f_c(\tau_k + (1 - a)u) + j\pi\gamma(au - \tau_k)^2\right\}\right\} du \\ &= \int_{-\infty}^{+\infty} \text{rect}\left(\frac{au - \tau_k}{T_p}\right) \cdot \text{rect}\left(\frac{\hat{t} - u}{T_p}\right) \\ &\quad \cdot \exp\left\{j\left(b_0 + b_1 u + b_2 u^2\right)\right\} du, \end{aligned} \quad (8)$$

where

$$\begin{cases} b_0 = -2\pi f_c \tau_k + \pi\gamma(\tau_k^2 - \hat{t}^2) \\ b_1 = -2\pi\gamma a\tau_k + 2\pi\gamma\hat{t} - 2\pi f_c(1 - a) \\ b_2 = \pi\gamma\left(a^2 - 1\right) \end{cases} \quad (9)$$

When $V_{Tran} \neq 0$, namely $a \neq 1$, there are additional first-order and second-order phase components induced by the velocity in the integration function of (8). The first-order phase component will give rise to the shift of range profile, while the second-order phase component will lead to the expansion of range profile.

III. HIGH VELOCITY MOTION COMPENSATION BASED ON ADAPTIVE PARAMETER ADJUSTMENT OF MATCHED FILTER AND ENTROPY MINIMIZATION

As mentioned above, the high velocity motion brings in aberration to the range profile and blurring the phase of ISAR imaging. To achieve high quality 1-D and 2-D imaging results, the high velocity motion compensation should be carried out firstly. The compensation methods for Dechirp processing are not valid since the phase item with high velocity cannot be separated after matched filtering. Hence, a new compensation method for IFDS data by adaptive parameter adjustment of matched filter and entropy minimization is proposed in this paper.

A. ADAPTIVE PARAMETER ADJUSTMENT OF MATCHED FILTER

Since the first-order phase component only lead to range profile shift and does not affect the 1-D imaging result. Hence, the compensation method focuses on the compensation of second-order phase component.

Firstly, the last phase item of (6) is compensated

$$\begin{aligned} s_{IF}(\hat{t}, t_m) &= s_{IF}(\hat{t}, t_m) \cdot \exp\left\{j2\pi f_c\left(1 - a\right)\hat{t}\right\} \\ &= \sum_{k=1}^{N} \sigma_k \text{rect}\left(\frac{a\hat{t} - \tau_k}{T_p}\right) \cdot \exp\left\{j\pi\gamma\left(a\hat{t} - \tau_k\right)^2\right\} \\ &\quad \cdot \exp\left\{-j2\pi f_c \tau_k\right\}. \end{aligned} \quad (10)$$

The expansion of range profile with high velocity is induced by the mismatching of matched filter essentially. The FMR is changed by the high velocity.

Applying Fourier transform of (10), one can have

$$S_{IF}(f,t_m) = \sum_{k=1}^{N} \sigma_k \frac{1}{|a|}\frac{1}{\sqrt{\gamma}}\text{rect}\left(\frac{f}{a\gamma T_p}\right)\exp\left\{-j\pi\frac{f^2}{\gamma a^2}\right\} \times \exp\left\{-j2\pi f\frac{\tau_k}{a}\right\}\exp\left\{-j2\pi f_c\tau_k\right\}. \quad (11)$$

To carry out matched filtering, the frequency response of the filter should be the following form

$$H(f,a) = |a|\frac{1}{\sqrt{\gamma}}\text{rect}\left(\frac{f}{a\gamma T_p}\right)\exp\left\{j\pi\frac{f^2}{\gamma a^2}\right\}. \quad (12)$$

Hence the impulse response is

$$h(\hat{t},a) = a^2\cdot\text{rect}\left(\frac{a\hat{t}}{T_p}\right)\exp\left\{-j\pi\gamma a^2\hat{t}^2\right\}. \quad (13)$$

It is just the matched filter with adaptive parameter adjustment. After matched filtering, the range profile can be achieved.

$$\begin{aligned} &s_{out}(\hat{t},t_m)\\ &= s_{IF}(\hat{t},t_m)\otimes h(\hat{t},a)\\ &= IFFT\left(S_{IF}(f,t_m)\cdot H(f,a)\right)\\ &= \sum_{k=1}^{N}\sigma_k a T_p \sin c\left\{a\gamma T_p\left(\hat{t}-\frac{\tau_k}{a}\right)\right\}\exp\left\{-j2\pi f_c\tau_k\right\}\\ &\approx \sum_{k=1}^{N}\sigma_k T_p \sin c\left\{B\left(\hat{t}-\frac{2R_k(t_m)}{c}\right)\right\}\\ &\quad\times\exp\left\{-j2\pi f_c\cdot\frac{2R_k(t_m))}{c}\right\}. \end{aligned} \quad (14)$$

It can be seen that the amplitude and phase distortion induced by high velocity is compensated and the range profile expansion is eliminated.

B. HIGH VELOCITY MOTION COMPENSATION BY ENTROPY MINIMIZATION

In order to carry out precise compensation, the velocity should be obtained as priori information. In real pulse radar experiment, it can be achieved from narrow band information. However, the precision cannot satisfy the compensation requirement. In this paper, the compensation is accomplished by entropy minimization of the range profile.

As can be seen from (14), only when the FMR is matched exactly between the echo and the filter can the ideal matched filtering and pulse compression be achieved. The range profile expansion is proportional to the FMR difference between the echo and the filter. Regardless of the value of the FMRs, the range profile expansion is minimized when they matching each other.

In statistics, entropy is used to indicate the evenness of probability distribution. 1-D entropy [9], [10] and 2-D entropy [11]–[13] have been introduced to the range

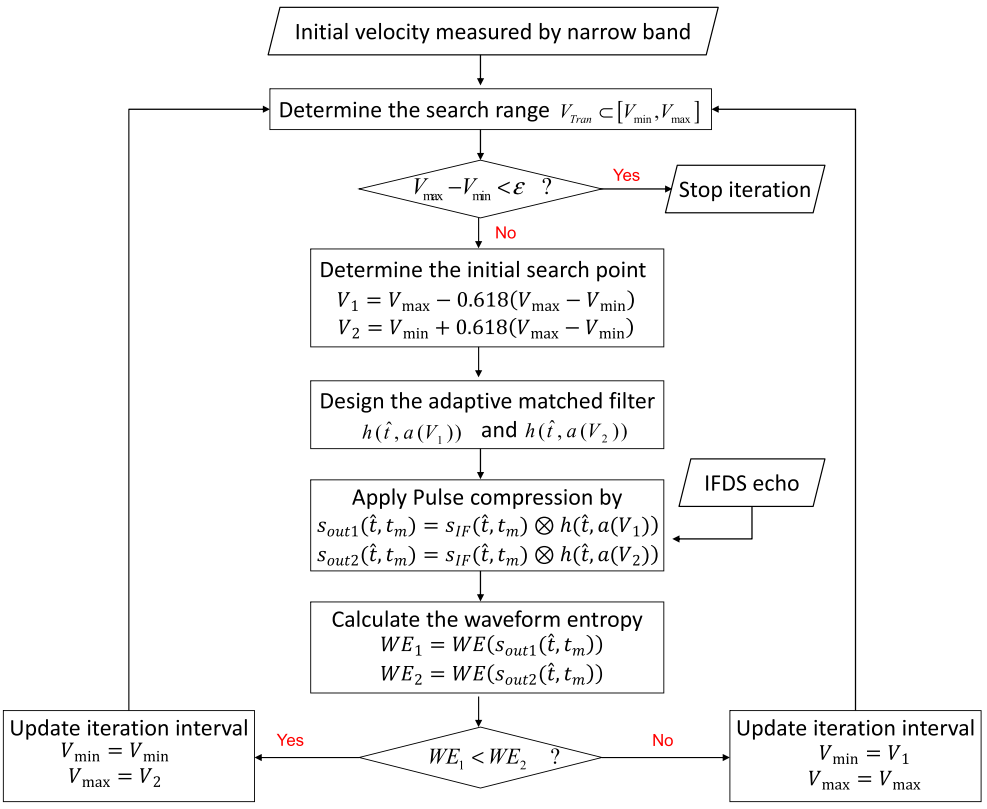

FIGURE 1. Schematic diagram of iteratively search.

alignment and phase correction in ISAR imaging. In this paper, the range profile entropy is introduced to judge the performance of high velocity motion compensation with different velocity. When the range profile is expanded seriously, the waveform entropy turns large. It turns small when the high velocity motion compensation is carried out with precise velocity.

Suppose the range profile vector is $s = [s_1, s_2, \cdots, s_M]^T$, where M is the sampling points in the range profile. Then the normalized vector can be written as $\tilde{s} = \left[\tilde{s}_1, \tilde{s}_2, \cdots, \tilde{s}_M\right]^T$, where $\tilde{s}_i = |s_i| / \sum_{i=1}^{M} |s_i|$. Hence the waveform entropy is defined as

$$WE = -\sum_{i=1}^{M} \tilde{s}_i \log_2 \tilde{s}_i. \tag{15}$$

In real experiment, the optimal velocity can be obtained when the waveform entropy of the compensated range profile is minimized.

$$\hat{a} = \min_a \left\{ WE\left(s_{out}(\hat{t}, a)\right)\right\} = \min_a \left\{ WE\left(s_{IF}(\hat{t}) \otimes h(\hat{t}, a)\right)\right\}. \tag{16}$$

C. ITERATIVE SEARCH FOR THE VELOCITY VIA GSS

In this section, a fast velocity search utilizing GSS [14]–[16] method based on waveform entropy minimization is adopted. GSS is very efficient in finding out the extreme of an objective function with unimodal [15]. After iterative search, the value of velocity and the matched filter and the ultimate compensated range profile can be obtained when the variety of the waveform entropy is under a given threshold.

Before applying the GSS method, the search region should be determined. In real experiment, the velocity measured by the narrow band can be used as prior information. Since the precision cannot satisfy the requirement of compensation, an error range is set around the measured velocity, constituting the search region which is depicted as $V_{Tran} \subset [V_{\min}, V_{\max}]$.

Suppose the search region length is $L = V_{\max} - V_{\min}$and the stopping threshold of the region length is ε, then the iterative search times can be obtained as

$$N_{IS} = \log_{0.618} \frac{\varepsilon}{L} = -4.78 \lg \frac{\varepsilon}{L}. \tag{17}$$

Consequently, GSS has very high efficiency and wide practicality.

The schematic diagram of the iterative searching process utilizing GSS method based on minimum waveform entropy is presented in Figure 1.

IV. EXPERIMENTAL RESULTS AND ANALYSIS

In this section, Simulation and real data is applied to test the influence of high velocity on 1-D range profile and 2-D ISAR imaging and the performance of the proposed compensation method.

A. THE INFLUENCE OF THE HIGH VELOCITY MOTION

Firstly, the influence of high velocity motion on 1-D range profile is displayed through a set of simulation data of a scattered point. The simulation parameters of radar system are set as follows, carrier frequency 9GHz, pulse width 200us, bandwidth 1GHz and sampling frequency 1.2GHz.

The single scattering point target model is shown in Fig. 2(a). In order to observe the effect of high velocity motion on pulse compression, different radial velocity of the target is set in simulation, such as $0m/s$, $1000m/s$, $3000m/s$, $5000m/s$. The range profiles achieved by direct matched filtering are shown in Fig.2(b). One can see that the expansion and shift of the range profile turns more serious as the radial velocity of the target improves.

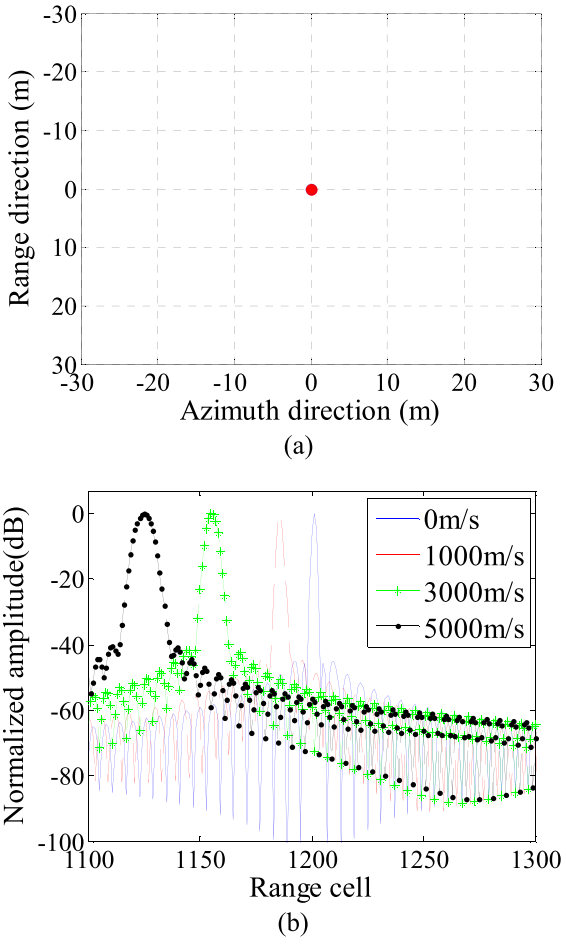

FIGURE 2. The influence of high velocity on 1-D range profile. (a) Target model. (b) Range profiles before compensation.

The high velocity motion of target brings the 1-D range profile expansion, and it destroys the phase information in the range profile sequences, which has a serious impact on 2-D ISAR imaging. The satellite scattering point model is used to simulate the influence of high velocity target motion on ISAR imaging. The satellite model consists of 97 scattering points of the same intensity, which is shown in Fig.3.

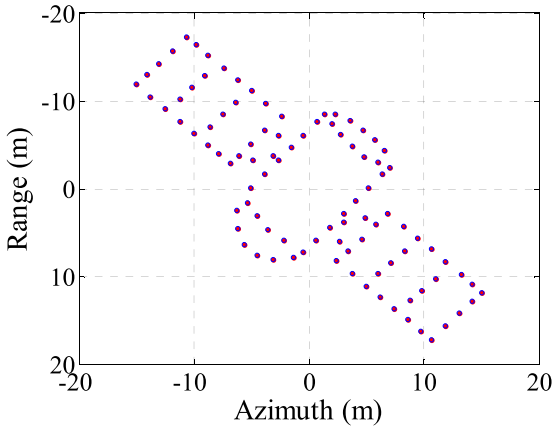

FIGURE 3. Satellite target model.

The IFDS echo sequences of the target with different radial velocities are simulated, containing 256 frame pulses. Assuming that the radial motion compensation has been accomplished and the target relative to the radar line of sight (LOS) can be equivalent to a standard turntable model. The target rotational velocity is set as $0.067 rad/s$, and the radar pulse repetition rate is 200Hz, and the turn angle of the target in the imaging integration time is $\Theta = 4.9°$.

The ISAR images after matched filter pulse compression and range-Doppler (R-D) imaging of the simulated data with different velocity are obtained respectively, as shown in Fig. 4(a) to (d). It can be seen that as the target radial velocity increases, the imaging results shift in the radial direction, and defocus appears in the range and azimuth direction as well. It is worth noting that when the target velocity is 0, the defocus turns more serious as the scattering points are far away from the rotational center. It is caused by the migration through resolution cell in the imaging process, which should be corrected to achieve more focused ISAR image.

In order to depict the effect of ISAR imaging more directly, the image contrast and entropy of different ISAR images are calculated. In general, the smaller the image entropy is, the better the focus is. The image entropy and image contrast of ISAR images with different velocity are given in the following table.

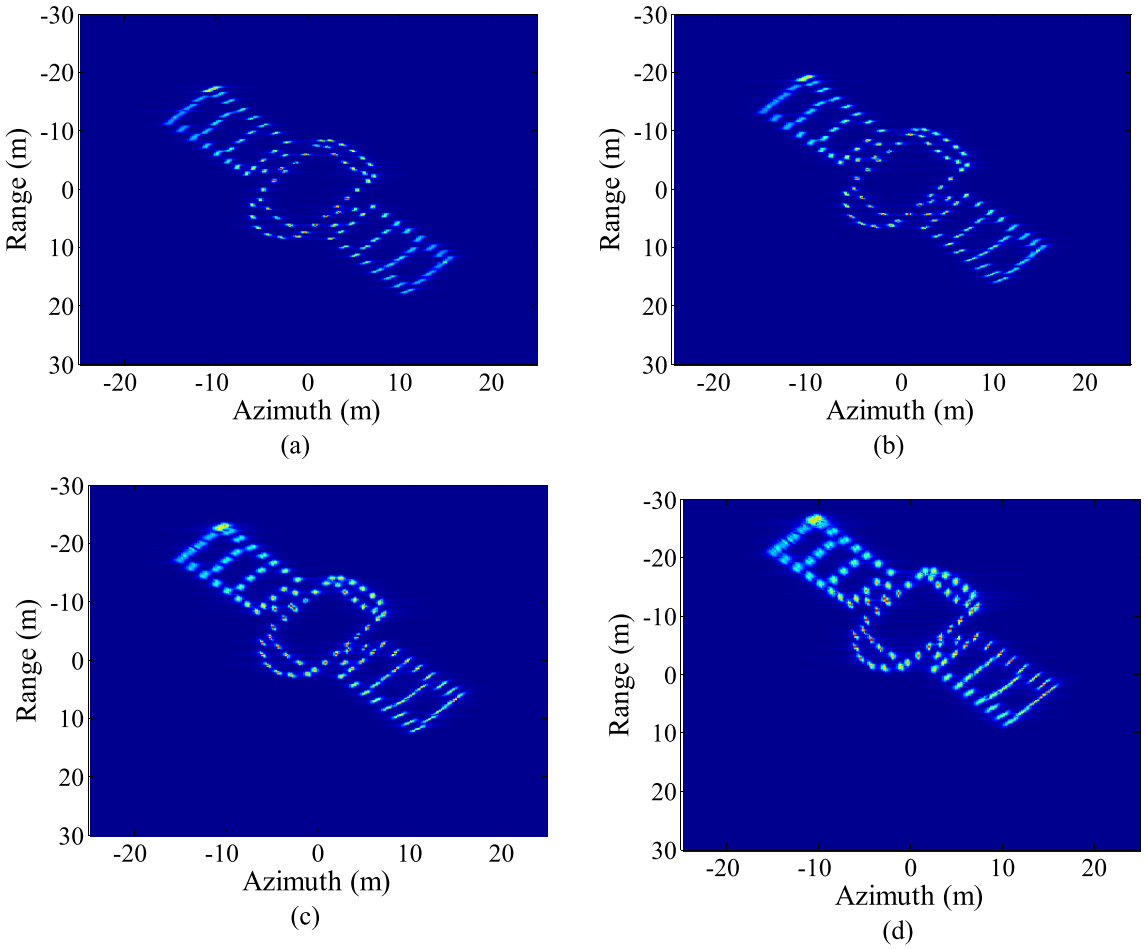

FIGURE 4. The influence of high velocity on 2-D ISAR image. (a) $V_{Tran} = 0$. (b) $V_{Tran} = 1000m/s$. (c) $V_{Tran} = 3000m/s$. (d) $V_{Tran} = 5000m/s$.

TABLE 1. The image entropy and image contrast of different ISAR images.

ISAR images with different velocity	Image entropy	Image contrast
0m/s	7.7345	22.3231
1000m/s	7.8171	21.3823
3000m/s	8.1418	17.9402
5000m/s	8.4264	15.3097

B. THE PERFORMANCE OF THE HIGH VELOCITY MOTION COMPENSATION METHOD

First of all, simulation data is used to verify the effectiveness of the proposed high velocity motion compensation method. Take the echo with 5000m/s as example. The initial search range is [4400 5500], and the iterative stopping threshold is 10. Fig. 5 shows the 1-D range profile imaging performance after applying the proposed compensation method. One can see that after compensation, the range profile expansion is weakened, while the range profile shift is also eliminated.

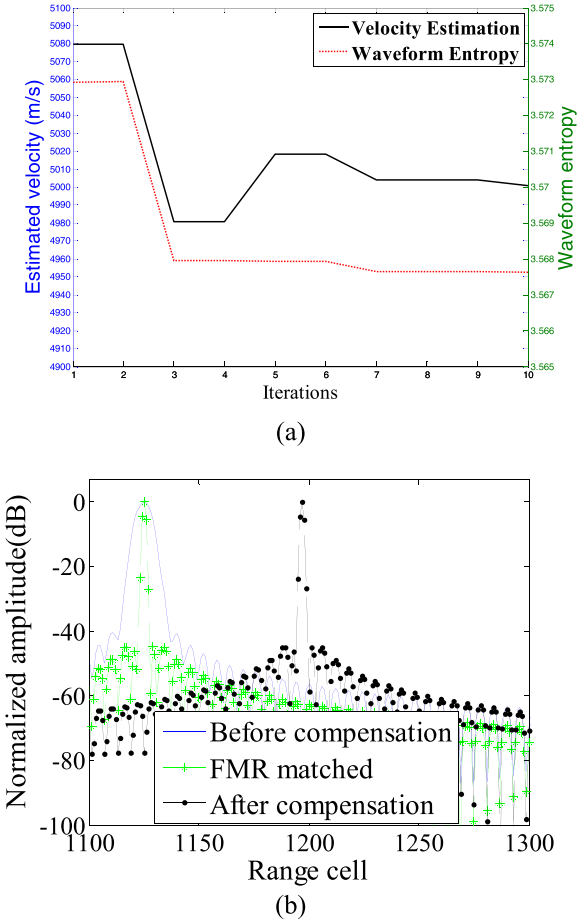

FIGURE 5. High velocity motion compensation of 1-D range profile. (a) The variation of waveform entropy and estimated velocity. (b) The range profile comparison.

Moreover, the iterative search times according to (17) is

$$N_{IS} = -4.78 \lg \frac{\varepsilon}{L} = -4.78 \lg \frac{10}{1100} \approx 10 \qquad (18)$$

As shown in Fig. 5(a), the estimate velocity achieves a finite convergence to the set parameter when 10 iterations are performed. Consequently, the waveform entropy reaches the minimum during the iteration.

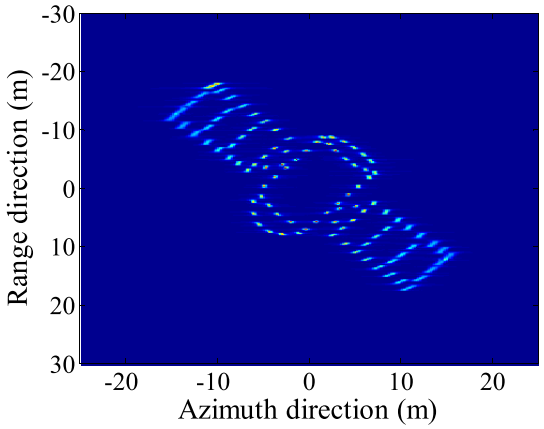

FIGURE 6. ISAR image of satellite target model after compensation.

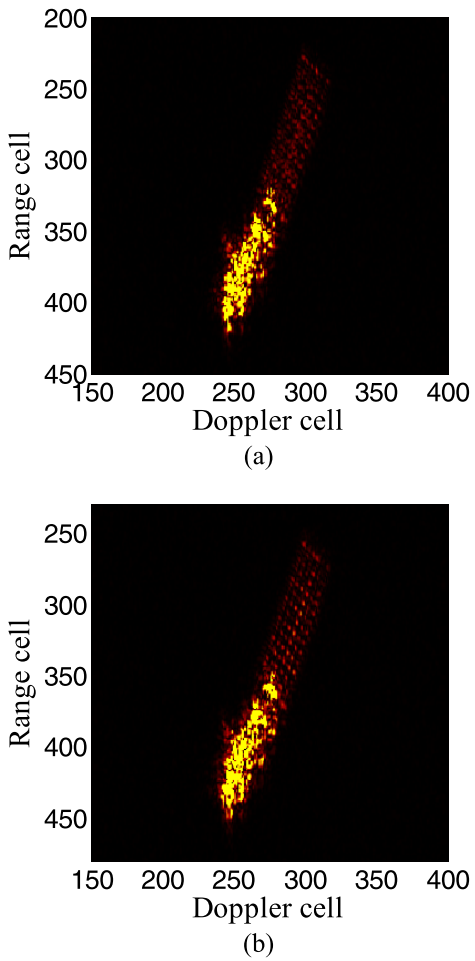

FIGURE 7. The compensation performance on real data. (a) ISAR image before compensation. (b) ISAR image after compensation.

Fig. 6 shows the ISAR image of satellite target model after compensation. It can be seen that the focusing effect of ISAR image is better after compensation. The expansion and shift in the range direction is eliminated. The image entropy and image contrast are 7.7527 and 22.1544, respectively. One can see that they are adjacent to the value without high velocity.

Moreover, the high velocity motion compensation is carried out for real radar measured IFDS data from a satellite. The ISAR images obtained before and after compensation are shown in Fig. 7. It can be seen that the image quality after compensation is obviously improved, especially in the satellite solar panel region. The image entropy and image contrast are calculated respectively, which are shown in Table 2.

TABLE 2. The image entropy and image contrast for real data.

ISAR images	Image entropy	Image contrast
Before compensation	9.98	21.24
After compensation	9.34	22.10

V. CONCLUSIONS

This paper proposes a new high velocity motion compensation method for IFDS data by adaptive parameter adjustment of matched filter and entropy minimization. The high velocity motion brings in aberration to the range profile and blurring the phase of ISAR imaging. Adaptive parameter adjustment of matched filter is designed to accomplish joint high velocity motion compensation and pulse compression. The Iterative search for the velocity utilizing GSS based on waveform entropy minimization is adopted to improve the efficiency.

REFERENCES

[1] C.-C. Chen and H. C. Andrews, "Target-motion-induced radar imaging," *IEEE Trans. Aerosp. Electron. Syst.*, vol. AES-16, no. 1, pp. 2–14, Jan. 1980.
[2] P. Hu, S. Xu, W. Wu, B. Tian, and Z. Chen, "IAA-based high-resolution ISAR imaging with small rotational angle," *IEEE Geosci. Remote Sens. Lett.*, vol. 14, no. 11, pp. 1978–1982, Nov. 2017.
[3] B. Tian, Z. Chen, and S. Xu, "Sparse subband fusion imaging based on parameter estimation of geometrical theory of diffraction model," *IET Radar, Sonar Navigat.*, vol. 8, no. 4, pp. 318–326, 2014.
[4] L. Zhang, M. Xing, C.-W. Qiu, J. Li, and Z. Bao, "Achieving higher resolution ISAR imaging with limited pulses via compressed sampling," *IEEE Geosci. Remote Sens. Lett.*, vol. 6, no. 3, pp. 567–571, Jul. 2009.
[5] Y. Liu, Z. Chen, N. Li, and S. Xu, "Wideband radar imaging for space debris based on direct IF sampling signals," *Proc. SPIE*, vol. 9250, p. 925014, Oct. 2014.
[6] A. Liu, X. Zhu, J. Lu, and Z. Liu, "The ISAR range profile compensation of fast-moving target using the dechirp method," in *Proc. IEEE Int. Conf. Neural Netw. Signal Process.*, Nanjing, China, Dec. 2003, pp. 1619–1623.
[7] C. He and D. Zhou, "High speed motion compensation based on the range profile," in *Proc. IEEE Int. Conf. Signal Process., Commun. Comput.*, Aug. 2013, pp. 1–4.
[8] K. F. Zhang, F. Wang, T. X. Dang, and Y. J. Zhao, "High speed motion compensation for range profiles," *Adv. Mater. Res.*, vols. 926–930, pp. 1720–1723, May 2014.
[9] P. Hu, S. Xu, and Z. Chen, "A robust sub-integer range alignment algorithm against MTRC for ISAR imaging," *Prog. Electromagn. Res. B*, vol. 77, no. 1, pp. 21–35, 2017.
[10] D. Zhu, L. Wang, Y. Yu, Q. Tao, and Z. Zhu, "Robust ISAR range alignment via minimizing the entropy of the average range profile," *IEEE Geosci. Remote Sens. Lett.*, vol. 6, no. 2, pp. 204–208, Apr. 2009.
[11] L. Xi, G. Liu, and J. Ni, "Autofocusing of ISAR images based on entropy minimization," *IEEE Trans. Aerosp. Electron. Syst.*, vol. 35, no. 4, pp. 1240–1252, Oct. 1999.
[12] L. Zhang, J.-L. Sheng, J. Duan, M.-D. Xing, Z.-J. Qiao, and Z. Bao, "Translational motion compensation for ISAR imaging under low SNR by minimum entropy," *EURASIP J. Adv. Signal Process.*, vol. 2013, no. 1, p. 33, 2013.
[13] P. Cao, M. Xing, G. Sun, Y. Li, and Z. Bao, "Minimum entropy via subspace for ISAR autofocus," *IEEE Geosci. Remote Sens. Lett.*, vol. 7, no. 1, pp. 205–209, Jan. 2010.
[14] C. H. Tsai, J. Kolibal, and M. Li, "The golden section search algorithm for finding a good shape parameter for meshless collocation methods," *Eng. Anal. Boundary Elements*, vol. 34, no. 8, pp. 738–746, 2010.
[15] Y.-C. Chang, "N-dimension golden section search: Its variants and limitations," in *Proc. Int. Conf. Biomed. Eng. Inform.*, Oct. 2009, pp. 1–6.
[16] J. A. Koupaei, S. M. M. Hosseini, and F. M. M. Ghaini, "A new optimization algorithm based on chaotic maps and golden section search method," *Eng. Appl. Artif. Intell.*, vol. 50, pp. 201–214, Apr. 2016.

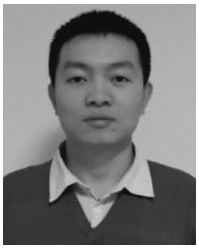

BIAO TIAN was born in Nanchong, China, in 1988. He received the B.S. and Ph.D. degrees in communication engineering from the National University of Defense Technology, Changsha, China, in 2011 and 2016, respectively. He is currently a Lecturer with the National University of Defense Technology. His current research interests include radar signal processing and imaging.

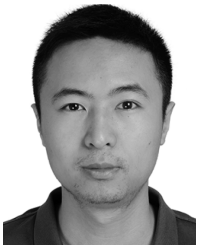

ZHEJUN LU was born in 1989. He received the B.S. and Ph.D. degrees in information and communication engineering from the National University of Defense Technology, Changsha, China, in 2011 and 2016, respectively. From 2014 to 2015, he was a Visiting Ph.D. Student with McMaster University, Hamilton, ON, Canada. He is currently a Lecturer with the National University of Defense Technology. His current research interests include target tracking and recognition.

YONGXIANG LIU (M'13) received the B.S. and Ph.D. degrees from the National University of Defense Technology (NUDT) in 1999 and 2004, respectively. He was an Academic Visitor with Imperial College London in 2008. Since 2004, he has been with NUDT, where he is currently a Professor with the College of Electrical Science. His current research interests include radar target recognition, time–frequency analysis, and micromotions.

XIANG LI (M'09) received the B.S. degree from Xidian University, Xi'an, in 1989, and the M.S. and Ph.D. degrees from the National University of Defense Technology in 1995 and 1998, respectively. He is currently a Professor with the College of Electrical Science, National University of Defense Technology. His current research interests include autotarget recognition, signal detection, and nonlinear signal processing.